

# 1 Introduction

The problem considered here is that of the solidification of an alloy starting from a single nucleus. In nature, this is an oft observed phenomenon, with the most readily available example being the growth of snowflakes in the atmosphere from a single spherical nucleus. Related to this is the dendritic solidification of alloys from a melt. The purpose of the project was to try and recreate a fast and efficient cellular-automaton based method to model the solidification pattern in alloys, first proposed in 2003 by Lee, et. al.<sup>1</sup>

## 2 Theoretical Background

### 2.1 One Dimension

The class of problem is traditionally called a moving-boundary or “Stefan” problem. And is usually formulated as follows:

Consider a region of space separated into two different “phases” by means of a boundary. The initial conditions are the shape of the boundary at time  $t = 0$  and the temperature field  $T(x, t)$  at  $t = 0$ . Notice that we have restricted ourselves to a one-dimensional problem here for simplicity. The solution to the problem would be  $T(x, t)$  at all  $t$  and  $x$  along with the solution to  $X(t)$  for all  $t$ . (Where  $X(t)$  is the position of the interface as a function of time)

Note that if we consider the solidification of an alloy, a further complication arises. The solidification of the alloy is dictated by both the diffusion of the temperature and the solute. If we consider that the temperature diffusion is much faster than the concentration diffusion, we will get a similar solution for the concentration field  $C(x, t)$  and the position of the interface  $X(t)$  because thermal diffusion and concentration diffusion are both governed by similar looking PDEs (source-less). And also a similar discontinuity in concentration

$$\frac{\partial T(\vec{x}, t)}{\partial t} = \alpha \vec{\nabla}^2 T(\vec{x}, t) \quad (1)$$

$$\frac{\partial C(\vec{x}, t)}{\partial t} = \kappa \vec{\nabla}^2 C(\vec{x}, t) \quad (2)$$

where  $\alpha$  and  $\kappa$  are the thermal diffusivity and the mass diffusivity coefficients respectively. Thus, we will continue to speak about the solidification of simple substances, limited by  $\alpha$ , as this will encompass the case of a solidifying alloy, with  $\alpha$  replaced by  $\kappa$  and  $T$  replaced by  $C$ . Note that the thermal diffusivity is given by  $\alpha = \frac{k_o}{\rho c_p}$ , where  $k_o$  is the thermal conductivity,  $c_p$  the specific heat, and  $\rho$  the density.

The restricted one-dimensional problem we are considering here can formally be stated as follows.

$$T(x, t) = \begin{cases} T(x, t) & : X(t) < x \quad t > 0 \\ T_o & : 0 < x < X(t) \quad t > 0 \end{cases} \quad (3)$$

$$\frac{\partial T}{\partial t} = \alpha \frac{\partial^2 T}{\partial x^2} \quad x > X(t), \quad t > 0 \quad (4)$$

$$T_o = T(X(t), t) \quad (5)$$

$$\frac{\partial T(x, t)}{\partial x} = -\frac{1}{\alpha} \frac{dX(t)}{dt} \quad (6)$$

$$T(x, 0) = \begin{cases} T_o & : x < 0 \\ T_1(< T_o) & : x > 0 \end{cases} \quad (7)$$

The differential equations to be satisfied by the system are (3) and (6), while the other equations serve as boundary conditions. We can obtain (6) from an energy conservation consideration, where the rate of heat given out freezing can diffuse away only as fast as the thermal gradient in the liquid phase. Note here that we ignore the thermal conductivity of the solid phase and also ignore the density change that typically accompanies a phase change. The problem then is as illustrated below, with a semi-infinite super-cooled liquid (below melting point) sitting in front of a solid phase moving towards it starting from  $x = 0$ . We seek to find the speed of the front movement.



Figure 1: *The problem under consideration. The black arrow indicates the direction of solidification*

As this is a case of a semi-infinite body with no characteristic length, we expect the existence of a solution in terms of a new scaled “similarity” variable, which is postulated to be given by

$$x^* = x/\sqrt{\alpha t} \quad (8)$$

This is from dimensional analysis or otherwise, and the similarity variable can be seen to be dimensionless. Under this transformation, (4) will reduce to

$$\frac{\partial^2 T}{\partial x^{*2}} = -\frac{x^*}{2} \frac{\partial T}{\partial x^*} \quad (9)$$

Assuming that  $T$  depends on the scaled variable  $x^*$  alone and not on  $t$  or  $x$  individually, this reduces to an ordinary differential equation whose solution is given by

$$T = A_1 + A_2 \int_0^{x^*} \exp\left(\frac{-x^{*2}}{4}\right) dx^* \quad (10)$$

Or, in less verbose notation,

$$T = A_1 + B_1 \operatorname{erf} \left( \frac{x^*}{2} \right) \quad (11)$$

Note that if (5) must be satisfied, then the  $x^*$  must be a constant (equal to  $T_o$ ) on the solid-liquid interface. Thus, it follows that

$$X(t) = 2\lambda\sqrt{\alpha t} \quad (12)$$

Where  $\lambda$  is a constant to be determined. Also note that once the constant is determined, the solution<sup>2</sup> can be found by applying the boundary condition (6).

## 2.2 Two Dimensions

In two dimensions, much of the results carry over in vector form, with the addition of a few complications. The first of these is the lowering of the melting point of the solid phase due to the curvature of the interface. This is called the Gibbs-Thompson phenomenon and can be explained with some thermodynamics. We first assume that the solidification is slow enough that we can make use of equilibrium thermodynamics to deal with it. Then, the free energies of the solid and the liquid phases are equal. The free energy of the solid phase must be corrected with an extra factor resulting from the interface energy.<sup>3</sup>

$$H_l - TS_l = H_s - tS_s + \frac{2 \times \gamma_{sl} \times V_{s,molar}}{r} \quad (13)$$

Where  $\gamma_{sl}$  is the surface energy between the solid and liquid phase,  $V_{s,molar}$  is the molar volume of the solid phase,  $r$  is the radius of curvature of the interface, and the rest of the symbols have their usual meanings. Rearranging terms, we arrive at

$$T_m = T_m^o - \frac{2 \times \gamma_{sl} \times V_{s,molar}}{r \times \Delta S} \quad (14)$$

Where the  $\Delta$  is across the solid and liquid parts,  $T_m^o$  is the melting temperature at a flat interface, and using the fact that  $\Delta H = T_m^o \times \Delta S$ . A similar result follows through for the chemical potential. A further complication is that the rate of solidification is faster along certain crystallographic directions. This can be modeled with a directional dependence of free energy. Other complications, such as kinetic under-cooling and density variations have been ignored. Even with this much simplification, though, this problem is hard to solve analytically.<sup>4</sup> This is where the numerous numerical methods come in. In this report, I will talk about the cellular automaton technique.

### 3 Cellular Automaton Techniques

The cellular automaton, in general, involves separating space into a grid of square “cells”. The cells then can have a “state” associated with them. The states of every cell in the grid change simultaneously at integer time intervals. The changes are based on a set of rules, which basically dictate the next state of a cell based on the current states of its neighbors. In the case of our simulation, the cells can be in three states: solid, liquid, or interface. We will first look at the one dimensional case.

#### 3.1 One Dimension

We consider a single line of square cells, and try and solve a similar problem as above, but we tackle the diffusion dominated solidification of an alloy. Each cell has an associated fraction of solid  $f_s$ . If  $f_s$  is zero, the cell is in a liquid state, with an associated concentration of solute in the liquid  $C_L$ . We assume that temperature is a constant through time and space during the simulation. Thus, from the phase diagram, the interface can have a range of concentrations, and the liquid phase can have any concentration greater than  $C_1$ . We fix the concentration of the solute in the solid phase to be  $C_s$ , and begin with the concentration analogue of an “undercooled” liquid, i.e., a liquid phase with a uniform initial concentration  $C_L^o < C_1$ .

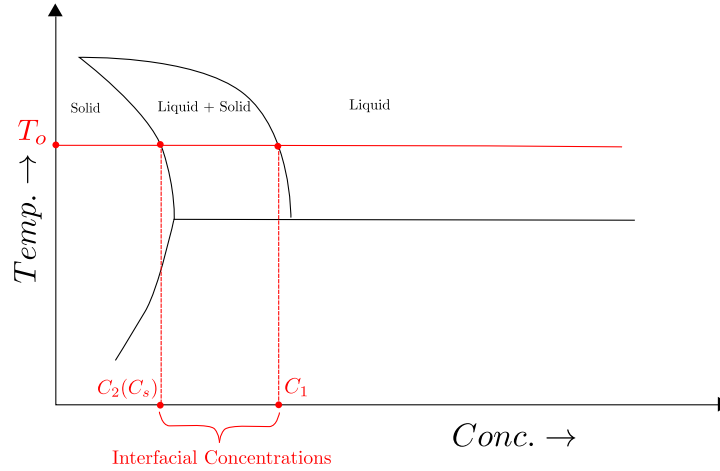


Figure 2: A simple phase diagram indicating various important quantities

Once  $f_s$  is non-zero, the cell becomes an “interface” cell. Only one cell can be an interface cell at any given moment. Here, the increase or decrease of the  $f_s$  is governed by a discretized version of (6), in the concentration from.

$$\frac{\Delta C \times \Delta x \times \Delta f_s}{\Delta t} = -\alpha \frac{C_{i+1} - C_i}{\Delta x} \quad (15)$$

Where  $\Delta C$  is the concentration difference denoted by  $C_1 - C_2$  in the diagram,  $i$  is the index of the interface cell,  $\Delta x$  and  $\Delta t$  are the space and time steps respectively, and  $\alpha$  is the usual diffusion constant. After solving this equation for  $f_s$ , we obtain the increase in the solid fraction at the interface. If the solid fraction reaches 1, the cell changes state to solid and the next liquid cell turns into an interface cell. We will always have an interface cell separating the two phases. Simultaneously, we also compute the diffusion of solute in the liquid phase, which can be obtained with discretised version of (4).

$$\frac{\Delta C}{\alpha \times \Delta t} = \text{second der}_x(\dots C_{i-1}, C_i, C_{i+1} \dots) \quad (16)$$

Where  $\text{second der}_x(C_i, C_{i+1} \dots)$  denotes any method to compute the discrete second derivative of the concentration at the  $i^{\text{th}}$  cell, the most common being the  $\frac{C_{i-1} - 2C_i + C_{i+1}}{\Delta x^2}$  scheme. We also ignore diffusion of the solute in the solid so that a constant concentration profile is maintained in the solid phase. The next section presents the results of the simulation.

## 4 Results

The simulation was run on a grid of size 240 cells, with various constants as set in the attached code. Because of the non-infinite nature of the grid, the stopping of the advance of the interface is expected after a certain interval of time. Also, any other analytical results derived are expected to hold only at the starting, where the edge of the grid has no effect. At the edge, we have used a no flux condition, so that concentration is conserved over space inside. The results of the simulation are shown below.

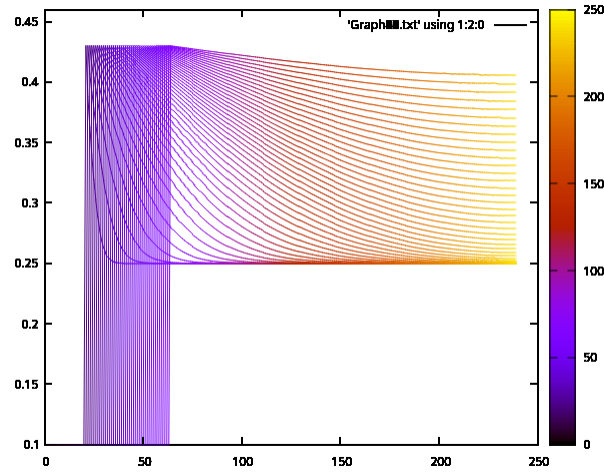


Figure 3: A graph showing the evolution of concentration profile with time

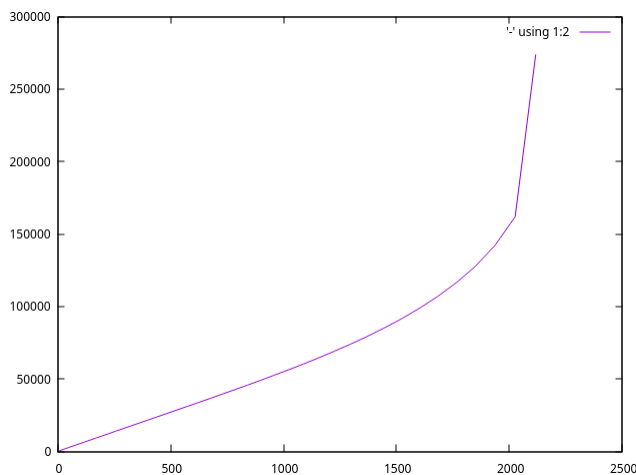


Figure 4: A plot of  $(\text{Position of interface})^2$  on the  $x$ -axis and  $(\text{time})$  on the  $y$ -axis

The position of interface plot is linear at the start, before the effect of the building up of solute at the end takes over, in close agreement with (12), which was derived analytically. The evolution of the concentration profiles reveal the reason behind the slowing down of the interface at the end: the solute concentration has become high enough that the liquid is no longer “undercooled” and unstable, and can coexist thermodynamically speaking, with the solid phase.

## 5 Future Work

We are currently working on a two dimensional cellular automaton, which will be of more practical use than the idealized one dimensional stefan problem solved above.

## 6 Constants Used in Simulation

```
#define LIQ_CON_START 0.25
// Starting conc. in liquid.
#define LIQ_CONC 0.43
// Conc. of solute in liquid (at Eq.)
#define SOL_CONC 0.10
// Conc. of solute in solid (at Eq.)
#define SIZE 240
// Size of the array on which sim is run.
#define DIFF_LI 0.009
```

```

// The diffusion const in liquid.
#define DEL_CON (LIQ_CONC - SOL_CONC)
// Difference in conc. of solute b/w liquid and solid at the relevant temp.
#define TIME 0.2
// The time step.
#define SPACE 0.2
// Space step.
#define INIT_INTERFACE 20
// Number of cells of solid, initially

```

## References

- [1] Wang, W., Lee, P.D. and Mclean, M., 2003. *A model of solidification microstructures in nickel-based superalloys: predicting primary dendrite spacing selection*. Acta materialia, 51(10), pp.2971-2987.
- [2] Carslaw, H.S. and Jaeger, J.C., 1959. Conduction of heat in solids. Oxford: Clarendon Press, 1959, 2nd ed, pp.287.
- [3] Kaptay, G., 2012. *The Gibbs equation versus the Kelvin and the Gibbs-Thomson equations to describe nucleation and equilibrium of nanomaterials*. Journal of nanoscience and nanotechnology, 12(3), pp.2625-2633.
- [4] Langer, J.S., 1980. *Instabilities and pattern formation in crystal growth*. Reviews of Modern Physics, 52(1), p.1.